NRC Research Press

ARTICLE

Landslide mobility analysis for design of multiple debris-resisting barriers

J.S.H. Kwan, R.C.H. Koo, and C.W.W. Ng

Abstract: Multiple debris-resisting barriers have been commonly used worldwide to mitigate debris flows in drainage lines. However, a well-developed methodology to assess the mobility of debris flows with consideration of the obstruction of the barriers does not exist. A free-field debris-flow condition that omits the presence of multiple debris-resisting barriers is commonly considered in design, although the effects of the barriers could be critical in determining the dynamics of the landslide debris including debris velocity and debris thickness. This paper proposes a staged debris mobility analysis that accounts for the effects of multiple debris-resisting barriers. The staged analysis adopts solutions of a depth-averaged debris mobility model. The input parameters of the analysis have been established from field data and laboratory test results. Rigorous numerical simulations of debris flows intercepted by multiple debris-resisting barriers have also been undertaken using the three-dimensional finite element program LS-DYNA to provide results for benchmarking the output of the staged analysis.

Key words: multiple debris-resisting barriers, landslide debris mobility analysis, debris flows, LS-DYNA.

Résumé : Les dispositifs anti-éboulement à barrières multiples ont été couramment utilisés à travers le monde pour réduire l'écoulement des débris dans les canaux d'évacuation. Cependant, on ne dispose pas de méthode permettant d'évaluer la mobilité des débris lors de leur écoulement et tenant compte de l'obstruction de ces dispositifs. Lors des phases de conception, on ne s'intéresse généralement qu'aux écoulements libres des débris sur le terrain sans tenir compte de barrières multiples anti-éboulement, alors que les effets de ces dernières influent beaucoup sur la dynamique des débris lors des glissements de terrain, en particulier sur la vitesse et sur l'épaisseur des débris. Le présent article présente une analyse par étape de la mobilité des débris, analyse qui tient compte des effets des dispositifs anti-éboulement à barrières multiples. Cette analyse s'appuie sur les résultats obtenus à l'aide du modèle de calcul de la mobilité moyenne en fonction de la profondeur. Les paramètres de départ de l'analyse ont été déterminés à partir des résultats obtenus sur le terrain ou lors d'essais en laboratoire. Des simulations numériques des écoulements de débris interceptés par les barrières multiples ont été réalisées de manière rigoureuse à l'aide du logiciel de simulation 3D LS-DYNA utilisant la méthode des éléments finis afin de pouvoir comparer les résultats ainsi obtenus à ceux de l'analyse par étape. [Traduit par la Rédaction]

Mots-clés : dispositifs anti-éboulement à barrières multiples, analyse de la mobilité des débris lors des glissements de terrain, écoulements de débris, LS-DYNA.

Introduction

Multiple debris-resisting barriers (referred to as multiple barriers herein) have been adopted in many countries to mitigate landslide hazards (Shieh et al. 2006; WSL 2008; Shum and Lam 2011). In general, multiple barriers comprise rows of single barriers installed at different strategic positions along the runout path of a given debris avalanche or debris flow. They are often built with a deposition area upstream to contain the debris. The barriers can be formed to different sizes and shapes to suit the topography, and a curved upstream surface may be provided to reduce the debris impact loading on the barrier (Shieh et al. 2006). Each row of single barriers is designed to retain a portion of landslide volume. Because of this, the scale of the individual barriers, in terms of structural requirements and retaining height, could be optimized to cope with the site constraints and could also be more effective in minimizing entrainment (Wong 2009).

Experience suggests that multiple barriers can be a practicable means to mitigate reasonably large debris avalanches and debris flows. Various international publications give guidance and recommend good practice for certain design aspects of multiple barriers. For example, CGS (2004) and NILIM (2007) provide guidelines for calculating retention volume of barriers, and SWCB (2005) recommends the minimum spacing between barriers. So far, however, there are no well-established design guidelines for assessing the effect of the presence of multiple barriers on landslide debris mobility.

Speerli et al. (2010) reported several debris flow flume tests to examine the dynamics of debris overflowing from small-scale ring-net barriers. A mixture of clayey gravelly sand and water was used in their tests. They observed that debris followed a ballistic projectile path after overtopping from the barrier and the debris was retarded upon impacting the flume bed at the landing position. Debris would then accelerate when it propagated downstream along the inclined flume. Glassey (2013), who evaluated the effectiveness of check dams installed in the Illbach channel in Illgraben, Switzerland, mentioned that energy gain and energy dissipation are involved in the process of debris overflowing from filled-up barriers and debris landing. Glassey suggested that the

Received 6 May 2014. Accepted 22 January 2015.

J.S.H. Kwan and R.C.H. Koo. Geotechnical Engineering Office, Civil Engineering and Development Department, Hong Kong SAR Government, Hong Kong.
C.W.W. Ng. Department of Civil and Environmental Engineering, Hong Kong University of Science and Technology, Clear Water Bay, Kowloon, Hong Kong.
Corresponding author: R.C.H. Koo (e-mail: raymondchkoo@cedd.gov.hk).

height of check dams should be at least the height of the debris flows.

Debris mobility assessment for the design of multiple barriers calls for consideration of salient features involved in the debris runout process, which include filling-up of barriers, overflowing from the barrier crest, and energy dissipation at the debris landing position. This paper presents an analysis of debris mobility for the design of multiple barriers based on pertinent field and laboratory studies. To facilitate the design of multiple barriers, a staged mobility analysis is proposed to provide a means for assessing debris mobility dynamics taking into account the obstructions of multiple barriers. A debris mobility model developed using the LS-DYNA computer program, calibrated against the Yu Tung Road debris flow, has also been adopted to undertake debris flow simulations for benchmarking the results of the staged mobility analysis.

Dynamic analysis of landslide debris

In the design of multiple barriers it has been assumed, due to the lack of a well-established methodology for assessing landslide debris dynamics, that the dynamics could be similar to that in the free-field conditions, i.e., presence of the multiple barriers is neglected. Wendeler et al. (2012) reported on a series of 13 barriers that was built along a drainage line to mitigate the debris flow hazard in Switzerland, and the barrier design was established on the basis of the maximum debris velocity observed in the field. On the other hand, some researchers (e.g., Remaître et al. 2008) have evaluated the influence of a series of filled-up barriers by considering variations in channel gradient. However, the analysis could not model reduction in debris volume and hence thickness due to debris retained by intermediate barriers.

In prevailing geotechnical practice, dynamic mobility models have been used in the design of debris-resisting barriers. With specific rheological parameters, numerical analyses can produce robust estimates of the dynamics of landslide debris for design purposes. Hungr et al. (2007) summarized details of various rheological and numerical models that were used in the debris mobility benchmarking exercise held in Hong Kong in 2007 and concluded that most of the common numerical models produced consistent results with the same specific rheological models.

Common numerical analyses for simulation of dynamics of landslide debris runout adopt a continuum model that was developed based on depth-averaged shallow-flow equations. The formulations are made with reference to columns of debris mass above a sliding surface. The DAN-W numerical debris runout model (Hungr 1995) adopts these type of formulations to simulate the post-failure motion of rapid landslides. A pre-defined volume of soil or rock changes into a fluid and flows downslope, following a path of a defined direction and width. The model implements a one-dimensional Lagrangian solution of the equations of motion and is capable of using several alternative rheological relationships (Hungr 1995). The model has been widely adopted in tengineering practice in Hong Kong for debris-resisting barrier design and landslide risk assessment purposes. Another numerical program, "debris mobility model" (DMM), that allows input of channel section geometry in a trapezoidal shape, was developed by Kwan and Sun (2006) based on modified formulations of Hungr (1995). This model has also been calibrated for used in Hong Kong. DAN-W is capable of simulating the ballistic flight of debris overshooting from vertical or subvertical runout paths, but DMM is not equipped with this function. Both DAN-W and DMM are Lagrangian models that discretize the landslide debris mass into interconnected slices in their computations. The process of debris filling-up barriers and the subsequent overflow may not be simulated realistically due to the connectivity of the slices assumed in the formulations of the models.

Eulerian continuum models viz. FLO-2D (O'Brien et al. 1993; Bertolo and Wieczorek 2005) and Kanako-2D (Liu et al. 2013) have been used for assessing dynamics of debris flows. According to Liu et al. (2013), Kanako-2D is able to simulate changes in elevation of a debris runout trail due to deposition or erosion. However, the simulation would not be applicable to situations where the flow velocity and flow depth change rapidly behind the barrier. In addition, simulation of the ballistic flight of debris from the crest of the barrier is not included in the formulations of the model. Similar to Kanako-2D, the dynamics of debris ballistic flight are not explicitly simulated by FLO-2D. The discharge above the barrier (or levee) is computed using the weir flow equation.

The above commonly used computer programs adopt a depth-averaged numerical scheme and the analyses are essentially two-dimensional. Three-dimensional continuum landslide mobility analyses have been undertaken by Crosta et al. (2007), who used an Eulerian-Lagrangian finite element code developed by Roddeman (2002). More recently, Yiu et al. (2012) reported the use of the three-dimensional finite-element package "Livermore Software – Dial-a-yield Nonlinear Analysis" (LS-DYNA) for landslide mobility assessment. LS-DYNA uses explicit time integration to study nonlinear dynamic problems. The package has been applied widely for stress and deformation analysis of structures subjected to impacts. The program handles scalar advection in an Eulerian grid and solves equations of motion based on an Arbitrary Lagrangian–Eulerian (ALE) description of the finite element method. Landslide debris is assumed to be elastoplastic, which follows the Drucker–Prager yield criteria. The computational domain was discretized into an array of hexahedral elements. The elements record the variables of acceleration, velocity, displacement, strain, stress, and kinetic energy of the landslide debris mass at various positions within the computational domain. Debris mass transport between elements follows the results of the ALE descriptions. The ground surface on which the landslide debris travels is modelled using rigid shell elements. The Coulomb frictional rule was assumed at the interface between the landslide debris and the shell surface. The LS-DYNA model was benchmarked against several well-documented laboratory and field studies, including the experiments of dry sand flows over irregular surfaces by Iverson et al. (2004) and the Yu Tung Road debris flow in Hong Kong (AECOM 2012). In the simulation of the Yu Tung Road debris flow, an additional damping force proportional to the square of the debris velocity was applied in the LS-DYNA analysis to retard the debris motion. This damping force accounts for the energy loss due to the turbulence of debris flows. Its magnitude has been estimated with reference to the velocity-dependent resistance of the Voellmy rheology (ARUP 2013).

Staged analysis for assessment of landslide mobility

The commonly used computer programs that adopt a depth-averaged scheme cannot simulate the entire process of debris filling up the retention zone of a barrier and subsequently overtopping the barrier. It is suggested that simulation of debris dynamics for the design of multiple barriers could be carried out based on a staged mobility analysis that adopts solutions of a depth-averaged Lagrangian model. The staged analysis comprises the following key steps:

1. Carry out debris mobility analysis using a suitable program (e.g., DMM or DAN-W) to simulate the dynamics of the landslide that travels from the source to the first barrier;
2. Use the results of the mobility analysis to determine the velocity at which the debris will launch into a ballistic flight from the crest of the barrier;
3. Calculate the geometry of the ballistic trajectory path and the debris velocity after landing;
4. Carry out debris mobility analysis to model the landslide debris travelling from the landing position to the next barrier; and

Fig. 1. Design parameters for assessing dynamic motion of landslide debris overflowing from barrier.

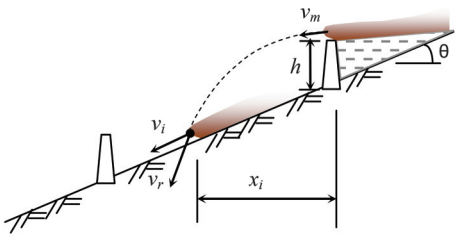

x_i = horizontal length of debris trajectory

v_m = debris launch velocity

v_r = debris velocity just before landing

v_i = debris velocity after landing, parallel to runout path

θ = inclination of runout path

h = height of barrier

5. Repeat steps 2 to 4 until the landslide debris reaches the terminal barrier.

When a landslide impacts on a barrier, a portion of the debris is trapped and retained behind the barrier, which results in a kinetic energy loss of the debris flow. Once the barrier retention zone is fully filled, the remaining debris launches into a ballistic flight from the crest of the barrier, carrying the kinetic energy of the remaining landslide debris. For a robust estimate of the length of the debris trajectory (x_i, see Fig. 1), the velocity at which the debris launches into a ballistic flight (see also step 2 above) may be taken as the maximum velocity of the remaining debris (v_m), assumed to be in the horizontal direction. v_m is taken as the maximum velocity parallel to channel slope at the location ($x = 0$, $y = 0$ in Fig. B1 of Appendix B) and assumed to act in the horizontal direction.

In the most common situations, the above assumption would be conservative and produce a more critical x_i, because the surface of the debris deposit behind an intermediate barrier is likely to be sloping at a lower angle than the natural channel. Kwan (2012) conducted a review of debris deposition angles behind barriers for the design of the retention capacity from field observations in many countries. The review showed that the range of deposition angles behind barriers is between 1/2 and 3/4 of the natural channel bed. However, there may be rare cases where the angle of debris deposition behind a barrier would exceed the inclination of the natural channel due to reasons such as excavation into the channel to form a steeper profile for the purposes of increasing the retention volume (Kwan 2012).

The v_m value can be obtained from the velocity output of the debris mobility analysis. For example, if a Lagrangian-type mobility model (e.g., DMM) is used, the mass blocks that would be trapped by the barrier would be those at the front of the debris chain with a volume equal to the retention capacity of the barrier, and the maximum velocity of the remaining mass blocks would be used for trajectory length calculation.

With the debris-launching velocity, v_m (in m/s) in the horizontal direction; height of barrier, h (in m); and inclination of the ground profile, θ (in degrees); the length of debris trajectory, x_i (in m), can be calculated using eq. (1) below, which is derived from the energy conservation principle (see Appendix B)

$$(1) \qquad x_i = \frac{v_m^2}{g}\left[\tan\theta + \sqrt{\tan^2\theta + \frac{2gh}{v_m^2}}\right]$$

where g is gravitational acceleration.

The equation above provides a reasonable estimate as compared with the results of flume tests (see Appendix A). If v_m is acting at an angle other than horizontal, the horizontal component of v_m can be input to eq. (1) for calculation.

The debris velocity just before landing, v_r (in m/s), is calculated based on the kinetic energy of the remaining debris and the kinetic energy gained in the drop from height as follows (see Appendix B):

$$(2) \qquad v_r = \sqrt{\frac{2[KE_r + m_r g(h + C_x x_i \tan\theta)]}{m_r}}$$

where m_r is mass of the remaining debris (in kg), KE_r is kinetic energy of the remaining debris (in J), and C_x is the correction factor for x_i.

Under common circumstances, each of the intermediate barriers would be designed to retain a certain portion of the debris flow. The remaining debris mass (m_r) relates to the amount of debris that cannot be trapped by the barrier, i.e., the total volume of debris before hitting the barrier less the barrier retention capacity that can be taking into account for the remaining debris from the upstream slope that will overflow the barriers. m_r and KE_r can then be obtained, based on the mass and velocity of the remaining mass blocks calculated from Lagrangian debris mobility analysis. If the barrier has been previously filled up completely by the debris materials, the retention capacity of the barrier should be ignored, and m_r and KE_r can be taken as the mass and kinetic energy of the entire landslide debris. The dynamics of subsequent overflow can still be analysed using the proposed staged analysis, e.g., for calculations of the overflow trajectory and debris mobility analysis between the debris landing location and the next barrier.

Essentially, the frontal portion of the debris flow travels at the highest velocity compared with the portion behind. Experience shows that debris flow velocity attenuates from the frontal portion, and the rate of attenuation becomes smaller towards the rear end of the debris flow mass. It is therefore expected that the velocity within the remaining debris (i.e., within the m_r) would not vary significantly, and the use of m_r in establishing v_r can be considered reasonable. However, if a short barrier height is used and the portion of debris retained is small, the use of frontal velocity of the remaining mass for establishing v_r would be more appropriate.

x_i is the maximum projectile distance that defines the landing position of the frontal portion of the remaining debris as it is calculated based on the maximum velocity of the remaining debris. As the velocity of debris varies, the correction factor C_x is applied to x_i in the equation for the sake of calculating the average projectile length of the overflow. Suggested values of C_x, corresponding to the ratio of rear velocity to frontal velocity of the remaining debris, are listed in Table 1. As field data for establishing C_x values are limited, the values presented in Table 1 are established based on a parametric numerical study of projectile lengths over different combinations of barrier height, debris velocity, and inclination of run-out path (see Appendix B). The program 2d-DMM has been calibrated in a number of landslide debris flow cases in Hong Kong and overseas including the 2008 Yu Tung Road debris flow considered in the illustrative example presented in this paper (Kwan and Sun 2006; Chan and Kwan 2012; Kwan et al. 2014). It is considered reasonable to use the well-calibrated program 2d-DMM to derive C_x for parametric studies.

Table 1. Suggested values of C_x.

Ratio of rear velocity to frontal velocity of remaining debris	C_x
<0.2	0.6
0.2–0.66	0.8
≥0.67	1.0

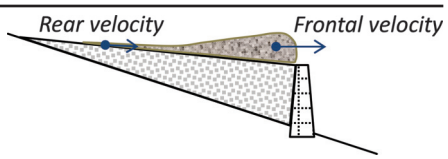

For carrying out the mobility analysis of landslide debris downstream as stated in step 4 above, an initial debris velocity is required. This velocity, v_i (in m/s), can be obtained by resolving v_r as shown below (for derivations of the equation refer to Appendix B):

$$v_i = Rv_r \cos\left\{\left[\tan^{-1}\sqrt{\frac{m_r g(h + C_x x_i \tan\theta)}{KE_r}}\right] - \theta\right\} \quad (3)$$

where R is the velocity correction factor.

To consider the velocity reduction due to the debris impacting on the trail at the landing position, a correction factor R should be applied to the above equation. The present study has analysed the results of the flume test by Choi and Ng (2013) with a view to determining a suitable value of R for design purposes.

The flume test was carried out using dry sand. Appendix A presents details of the test set-up. Instrumentation of the test included high-speed cameras, laser sensors, and photo sensors. High-resolution images were captured during the test to investigate the dynamics of debris impacting and filling up the rigid barrier, then launching into a ballistic flight from the crest of the barrier and resuming its travel on the flume bed upon landing (see figure presented in Appendix A). The image data have been interpreted by the present study using the particle image velocimetry (PIV) technique developed by White et al. (2003) for estimating the velocity reduction at landing.

Typical PIV results are presented in Fig. 2, which shows the velocity at the instant about 0.5 s after the sand had impacted on the barrier. The sand overflowed from the crest of the barrier at a velocity of about 1 m/s and then launched into a ballistic flight. It followed a projectile trajectory and finally landed on the flume bed at a maximum distance of 0.21 m downstream of the barrier. Due to the release of the potential energy, the sand flow accelerated along the trajectory path. The maximum velocity was up to about 1.8 m/s immediately before landing. Upon landing, the sand flow travelled along the flume bed. The sand flow velocity was reduced after landing. The ratio of the velocity parallel to the flume bed after and before impact has been determined at various times during the test. This velocity ratio ranged from about 0.3 to 0.5. Appendix A presents detailed interpretation of the test results.

It should be noted that dry sand is frictional and develops high flow resistance at the impact point, where the normal momentum of the falling mass creates a large normal force. In the case of saturated materials in the field, however, such an impact may create high pore-water pressure in the debris, resulting in low effective normal stress and hence small flow resistance.

Flume tests involving ballistic trajectory of dry granular flow comprising rock blocks has been conducted by Yang et al. (2011). The rock blocks used in their experiments were of dimension of up to 0.1 m. According to Yang et al. (2012), the granular flows in their tests involved rolling and bouncing of large granular particles. These flume tests may replicate the dynamics of debris avalanche. They observed that the granular flow was subjected to velocity reduction upon landing on the flume bed. Yang et al. (2012) reported that the velocity immediately after and before landing ranged from 0.41 to 0.75 with an average of 0.65.

Head loss of wet debris flows dropping from height has been studied by Chen et al. (2009). They carried out measurements along debris transport channels equipped with drop structures, and suggested a formula for estimation of head loss of debris flow dropping from height. The velocity of the debris flows reported by Chen et al. (2009) ranged from 3 to 6 m/s and the debris transport channels in their study were gently inclined (about 10°). Based on the suggested formula, it can be estimated that the ratio of the velocity in the direction of the downstream channel after and before landing is in the order of 0.3 for a debris flow of thickness ranging from 0.5 to 1.5 m with a drop height of 2 to 4 m.

In addition to the above, data reported by Glassey (2013) and videos of Illgarben debris flows (available at http://www.wsl.ch/fe/gebirgshydrologie/massenbewegungen/prozesse/murgang/videos/index_EN, http://www.youtube.com/watch?v=tjWZTP3u9d4, http://www.youtube.com/watch?v=OUtZVn2NwrY, and http://www.youtube.com/watch?v=tjWZTP3u9d4) have been reviewed. Quantitative data have been determined for investigation of the R factor. Overall, the range of the R factor is between 0.3 and 0.75. The results are systematically presented in Table 2. The value of R correlates with channel base materials. It is noted that the R factor for debris impacting on a hard flume channel base varied between 0.5 and 0.7. However, when the flume channel filled up with debris, the R factor could reduce to a range of 0.3 to 0.5. This phenomenon of R factor reduction is also observed in the field studies in China and Illgraben when the channel base is filled up with loose materials or debris. Comparisons between dry sand flows and wet debris flows show that ranges of the R factor are similar. It is expected that high water content would give a higher value of the R factor because water would act as a lubricant. However, the turbulence effects brought about by the water may contribute energy loss. The field cases in Illgraben with high water content of debris flows also give a similar range of the R factor between 0.4 and 0.7, except after the channel base is filled up with debris. All in all, the ratio of velocity parallel to debris trail after and before landing could range from 0.3 to 0.75. The flow dynamics of debris impacting on the ground are complex. More importantly, the actual water content, particle-size distribution, and characteristics of the channel bed at the landing location that affect the velocity reduction could vary significantly. It is not easy to define a value of R precisely. In view of the large uncertainties involved, a value of R on the high side — 0.7 — is recommended.

Debris mobility analysis to model the dynamics of landslide debris travelling from the landing position to the next barrier would be carried out as per step 4 above. x_i, as mentioned above, gives the initial position at which the debris mobility analysis would commence, and v_i gives the initial velocity of the debris for the subsequent analysis. Two other parameters, i.e., debris length (x_d) and debris thickness (h_m), are required for carrying out the analysis. The length of the debris, x_d, is assumed to be the same as that of the remaining debris before the overflow (i.e., the length of mass blocks that would not be trapped by the barrier). If the length of debris is greater than the length of debris trajectory (i.e., $x_d > x_i$), the debris is taken to extend backward from the point of landing to beyond the barrier for calculation purposes. Though this is an idealization, it is more robust for design as the debris would start motion again with a higher potential energy. An additional reason for adopting x_d as opposed to x_i is that the latter would have led to greater initial debris thickness for the subsequent mobility analysis, which could have resulted in unrealistic basal resistance particularly for a Voellmy rheological model (Hungr 1995).

Fig. 2. Debris overflows from crest of rigid barrier.

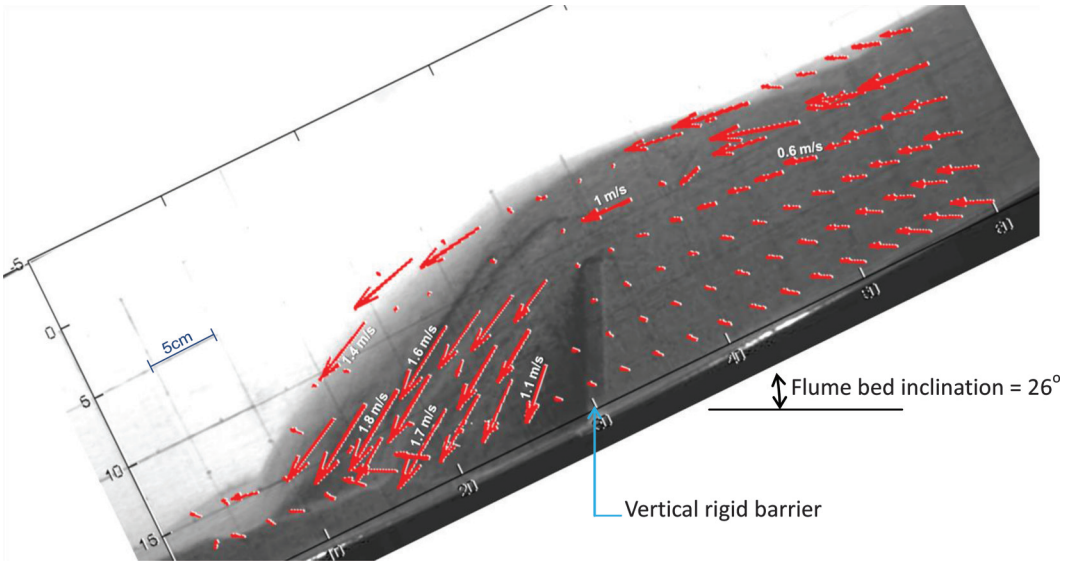

Table 2. *R* factor determined from the field and laboratory tests.

Case	Water content	Bedding	Water in channel at impact	Channel gradient (°)	*R* factor
1. Bouldery granular flow (Yang et al. 2011)*	Dry	Hard flume base	No	10	0.4–0.7
2. Debris flow mixture from clay to gravel (Speerli et al. 2010)*	25%–30% by mass	Hard flume base	No	9–14	0.5–0.7
3. Sand flow (Choi and Ng 2013)*	Dry	Hard flume base (first surge)	No	26	0.5
		Sand base	No	26	0.3–0.4
4. Watery debris flow (Chen et al. 2009)†	High	Soft channel base	Yes	10	0.3
5. Bouldery granular flow‡	50% by volume	Gravelly base (1st surge)	Yes	5–10	0.4–0.7
		Bouldery deposit (rear surges)	Yes	5–10	0.3–0.5

*Experimental flume tests.
†Field tests.
‡Field tests (information from the Illgraben debris flow observations in Switzerland on 3 June 2000, 28 June 2000, 22 July 2013, and 28 July 2014).

Debris thickness, h_m, upon landing can then be determined based on the volume of the remaining debris and width of the runout trail. To simulate a greater debris frontal thickness than observed normally, it is suggested that the maximum thickness of the remaining debris at the debris front should be adopted. The thickness of the frontal one-fifth of the mass blocks is taken to be the maximum thickness of the remaining debris (i.e., if 50 mass blocks are used to model the whole landslide debris, 10 mass blocks at the frontal position are assigned to have the maximum thickness of the remaining debris). The debris thickness is then assumed tailing off at a profile that corresponds to a volume of the remaining debris.

With the four initial conditions viz. v_i, x_i, h_m, and x_d as established above, a separate landslide debris mobility analysis can start off from the landing position to the barrier downhill. The impact velocity of landslide debris at the downhill barrier can be then calculated.

Sensitivity analyses of barrier height and other parameters

Sensitivity analyses have been carried out for different combinations of barrier height from 1 to 5 m and a range of launching flow velocities (v_m) from 4 to 10 m/s using the proposed staged analysis (see eqs. (1) to (3)) to investigate the effect on the debris velocity after landing (v_i). A slope inclination between 5° and 30° has been assumed. It is observed that a multiple barrier system could be more effective in dissipating energy if short barriers are used, as short barriers limit the energy gain of landslide debris during overflows. Another observation is that the ratio of v_i/v_m is not sensitiv in the ranges of the parameters considered. Only 15% variation in v_i/v_m is observed.

Application of staged mobility analysis

The application of the staged mobility analysis is demonstrated through an illustrative example pertaining to the design of debris-resisting barriers for the protection of Yu Tung Road, Hong Kong, from debris flow hazards. On 7 June 2008, a sizable channelized debris flow involving an active volume of about 3400 m^3 occurred in a natural hillside catchment above Yu Tung Road (a video showing the debris flow event is available at http://youtu.be/R2uTKyK1c9k). Different pulses are observed in the video that characterize the mobility of the debris flow. The proposed staged analysis can be applied to analyse the dynamics of the overflow and debris dynamics between the landing location and the next barrier. A detailed geotechnical investigation of the event is reported by AECOM (2012). The debris flow is referred to as Landslide No. 25 (LS08-241), Catchment No. 30 in AECOM's report.

Figure 3 shows the catchment and the section of the natural drainage line, taken after the debris flow event. The debris flow was a result of a massive landslide with a 2350 m^3 failure volume at the head of the drainage line. Severe rainfall was one of the contributing factors of the landslide. The landslide materials entered into the incised drainage line (see also Figs. 3 and 4), mixed with surface runoff and developed into a debris flow with an

Fig. 3. Catchment of Yu Tung Road debris flow.

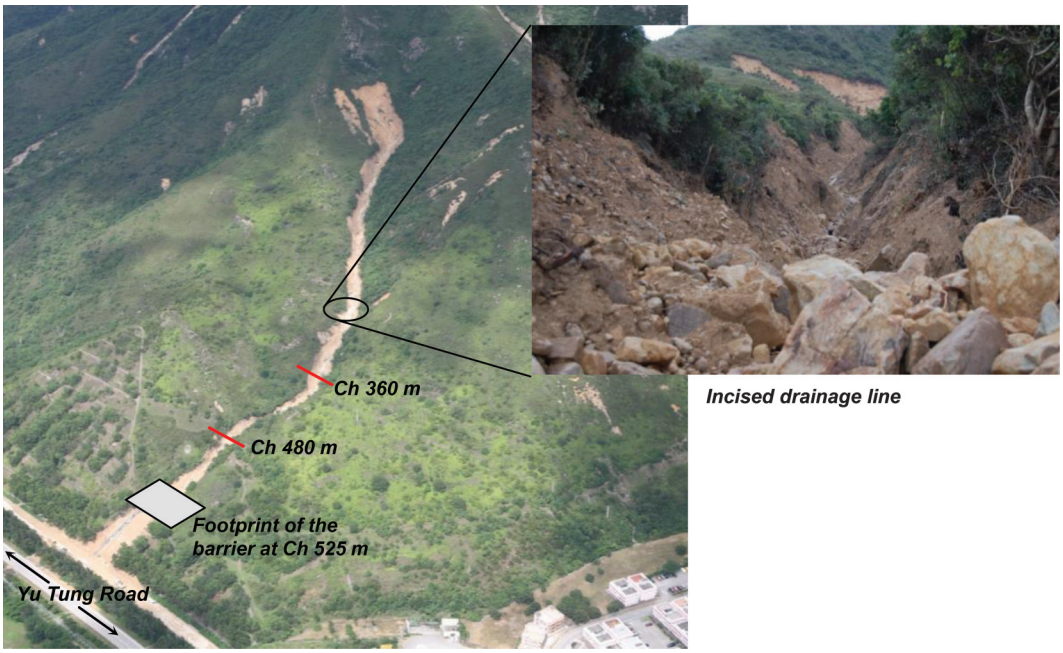

additional volume of 1000 m^3. The debris flow travelled about 600 m and disrupted the traffic of Yu Tung Road immediately downstream of the drainage line outlet.

Before the debris flow, the landslide risk of the catchment had been identified and the design of a rigid debris-resisting barrier was underway. (The construction of the rigid barrier is now complete.) The barrier is located at the outlet of the drainage line (chainage Ch 525 m; the chainage starts at the crown of the landslide scar). The design debris-retention volume was taken as 3500 m^3. To achieve this retention volume, a 7 m high barrier wall was built. Debris mobility analysis was carried out with an assumption that a volume of 3500 m^3 ground mass would detach at the head of the drainage line to establish the debris impact velocity and debris thickness for design of the rigid barrier. A detailed back-analysis of the presented Voellmy parameters has been carried out by Kwan et al. (2012) to best-fit the observation of the Yu Tung Road case. Voellmy rheological parameters comprising a basal friction coefficient of 0.14 (tan φ_b , where φ_b is apparent basal friction angle (= 8°)) and turbulence coefficient of 500 m/s^2 (Kwan et al. 2012) were adopted in the debris mobility analysis. The design debris impact velocity and debris impact thickness for the barrier at Ch 525 m are 8 m/s and 2.1 m, respectively.

To demonstrate the applicability of the staged debris mobility analysis, it is assumed that two intermediate barriers at Ch 360 m and Ch 480 m were proposed and a staged approach is used for calculation of the impact debris velocity and impact debris thickness of the two intermediate barriers. This serves as an example to illustrate how the proposed staged approach is used. The height of the intermediate barriers is 3 m. The corresponding retention volumes calculated following the guidelines stated in CGS (2004) are 780 and 700 m^3. With the two intermediate barriers, a smaller design debris retention capacity of the terminal barrier at Ch 525 m would be required, and the barrier wall height is estimated to be 4 m. The number of intermediate barriers and the barrier height adopted in this illustrative example have not been optimized. In a real design exercise, the number and height of barriers should be determined with consideration of the design retention volume, potential visual impact, cost effectiveness, site accessibility, and actual topography.

The staged mobility analysis was carried out using debris mobility program 2d-DMM (the latest version of 2d-DMM allows for debris mobility analysis with an initial debris velocity specified as required in the proposed staged analysis). The analysis started with a debris volume of 3500 m^3 at the landslide source area (i.e., the head of the drainage line) with a maximum thickness of about 3 m. Figure 4 shows the runout profile adopted in the mobility analysis. The vertical scale of the landslide source thickness and barrier height has been exaggerated by 50 times for clarity. The same rheological parameters as those of the conforming design were used. The analysis ran until the debris reached the first intermediate barrier at Ch 360 m. Using eqs. (1) to (3), the initial conditions for the next stage of landslide mobility analysis were established. The next stage of analysis was then carried out commencing downstream of the barriers. The procedure repeated until landslide debris reached the terminal barrier at Ch 525 m. With the staged analysis, the velocity and thickness of debris approaching each of the barriers were calculated. Key results and the initial conditions involved are summarized in Table 3.

The staged analysis aims to assess the dynamics of the landslide debris with consideration of the obstruction of multiple barriers. According to the results of the analysis, the design debris impact velocity and thickness for the terminal barrier are 7.3 m/s and 1.1 m, respectively. Comparing with the design values established for no intermediate barriers, i.e., 8 m/s and 2.1 m, the analysis shows that the intermediate barriers could lead to a reduction of 9% in debris velocity and 52% in debris thickness.

However, construction of the first intermediate barrier could be a technical challenge because the barrier is required to resist a relatively high impact velocity (12.0 m/s) and great impact thickness (2.8 m). This highlights the importance of location selection for building intermediate barriers. Ideally, intermediate barriers should be positioned at broad and flat portions of the drainage line, which provide favourable conditions for slowing down landslide debris.

To ensure the function of debris retention, routine maintenance, e.g., regular debris clearance, would be needed. If it is assessed to be appropriate, i.e., the multiple barriers function as a series of check dams, clearance of landslide debris would not be required. The filled barriers would contribute to a less-steep runout profile that helps to reduce mobility and runout distance of any subsequent landslide events.

Fig. 4. Runout profile of mobility analysis.

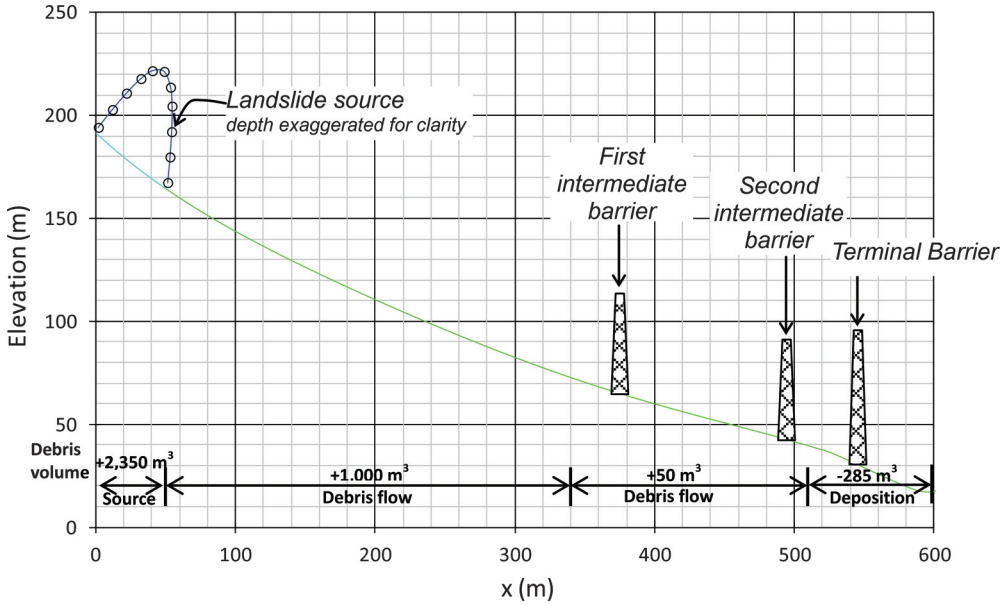

Table 3. Key results and initial conditions involved in the staged mobility analysis.

	Design parameters		Initial conditions for next stage analysis starts at downstream of barrier			
Barrier	Debris approaching velocity (m/s)	Debris approaching thickness (m)	v_i (m/s)	x_i (m)	h_m (m)	x_d (m)
First intermediate (Ch 360 m)	12.0	2.8	10.4	15	3	192
Second intermediate (Ch 480 m)	8.3	1.9	6.1	7	3	192
Terminal (Ch 525 m)	7.3	1.1	—	—	—	—

Benchmarking with LS-DYNA analysis

A three-dimensional debris mobility analysis using the LS-DYNA computer program has been carried out. The analysis produces data for benchmarking the results of the staged mobility analysis. The LS-DYNA model developed by Yiu et al. (2012) is adopted. The program handles scalar advection and solves equations of motion based on an ALE description of the finite element method. The runout distance of the Yu Tung Road debris flow exceeds 600 m and the width of some sections of the corresponding runout trail is over 30 m. The computational domain is discretized into an array of uniform hexahedral elements of dimensions 2 m (wide), 2 m (long), and 0.5 m (deep). Over 930 000 elements are used in the model.

Drucker–Prager yield criteria are assumed to describe the internal rheology of the debris flow. Key parameters that define the properties of the debris flow materials are listed in Table 4. ARUP (2013) reported that the analysis result is not sensitive to Poisson's ratio (υ). A typical value of υ of 0.3 is adopted.

The bulk density (ρ) and stiffness parameters, including E and υ, haved been found not to be sensitive to the results of the analysis (ARUP 2013). Typical values commonly adopted in geotechnical analysis for design purposes are therefore assumed (Kwan et al. 2012). The Yu Tung Road debris flow was watery as shown in the video record and the sedimentology of the event could mainly comprise sandy and coarse materials (AECOM 2012). In theory, it is a cohesionless material. However, specification of a nonzero value of cohesion is required for LS-DYNA analysis. Therefore, a nominal value, or a very low value of cohesion — 0.1 kPa — is assumed. The internal friction angle (φ_{int}) affects the mobility of the landslide debris in the LS-DYNA analysis, and has been back-calculated based on the velocity determined from the video record and the super-elevation data mapped on site (see Fig. 5) based on the best-fit model parameters.

Table 4. Key parameters of material properties.

Material property	Parameter
Bulk density, ρ (kg/m³)	1900
Elastic modulus, E (MPa)	10
Poisson's ratio, υ	0.3
Internal friction angle, φ_{int} (°)	15
Apparent cohesion, c (kPa)	1

In addition to φ_{int} , resistance to landslide debris motions modeled in the analysis affects the simulated debris mobility. The resistance applied in the model comprises (*i*) basal friction at the interface of the landslide debris and the surface of the runout trail and (*ii*) damping force proportional to the debris velocity. The basal friction is assumed to be of the Coulomb type and is proportional to the normal stress acting at the debris–ground interface. A basal friction coefficient (tan φ_b , where φ_b is 8°) of 0.14, the same as for the 2d-DMM analysis, is adopted. The damping force (F_d) is calculated as per eq. (4)

$$F_d = \xi_d m v^2 \quad (4)$$

where ξ_d is the proportional constant, m is mass of debris, and v is debris velocity.

This damping force is applied to simulate the energy dissipation due to turbulence. In depth-averaged calculations, similar resistance, proportional to v^2, is considered in the Voellmy rheology

Fig. 5. Frontal debris flow velocity versus chainage using best-fit model parameters.

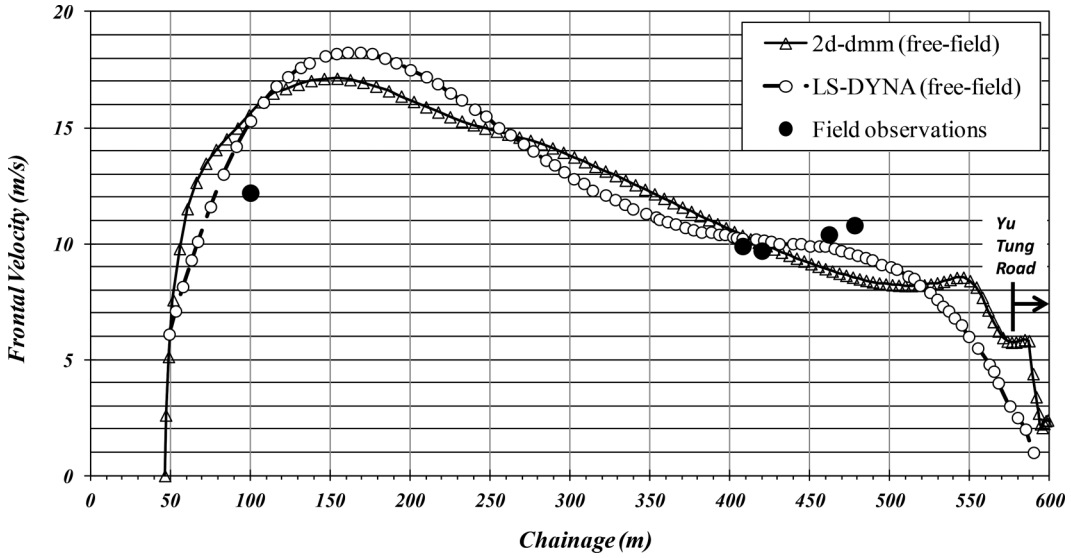

(Hungr 1995). The turbulence resistance (F_{turb}) in the Voellmy rheology is defined as

$$F_{turb} = mgv^2/\xi h \quad (5)$$

where g is gravitational acceleration, ξ is the turbulence coefficient, and h is debris thickness.

Voellmy rheology has proven to produce reasonable simulations of channelized debris flows (GEO 2011). The damping force applied in LS-DYNA analysis is therefore established with reference to the Voellmy rheology. The accelerations (or decelerations) resulting from F_d are pegged to that of F_{turb} (i.e., $F_d/m = F_{turb}/m$). It follows that

$$\xi_d = g/\xi h. \quad (6)$$

According to GEO (2011), ξ should be taken as 500 m/s² for modeling channelized debris flows for design purposes. Using eq. (6) and on the basis of the field mapping results that the average debris thickness of the debris flow event is in the order of magnitude of 2 m, ξ_d for the LS-DYNA analysis is taken as 0.01 m^{-1}.

Figure 5 shows the frontal debris flow velocity of the Yu Tung Road debris flow calculated by 2d-DMM and LS-DYNA. Both numerical models produced comparable results that generally matched the debris velocity determined based on the video record and super-elevation data mapped in the field. The differences would have been caused by the localized channel surface conditions, which have not been modelled explicitly. Also, the water content of the debris flow may also affect the turbulence effect on the velocity at certain locations with various topography conditions. It is difficult to obtain sufficient original specific information throughout the debris flow path after the event has occurred. In light of this information, a constant best-fit set of rheological parameters has been applied throughout the debris flow profile. Also, the field observations were estimated from the super-elevations instead of instrumental measurements, which could be associated with some degrees of uncertainty. 2d-DMM and LS-DYNA adopt different numerical strategies. 2d-DMM is developed based on a depth-averaged approach, whereas LS-DYNA is a full three-dimensional analysis with consideration of the yield criteria of the materials being modelled. The 2d-DMM analysis requires a pre-defined debris trail width whereas LS-DYNA does not. These factors may also contribute to the difference between the two simulation results. The internal friction angle (φ_{int}) used in the LS-DYNA analysis is 15°. The LS-DYNA analysis is undrained in nature and φ_{int} should be regarded as an apparent friction angle that incorporates the effects of pore-water pressure. Given that the debris flow is watery, this back-calculated internal friction angle (i.e., 15°) is of a reasonable order of magnitude. In addition to debris velocity, the LS-DYNA analysis reproduced a debris flow length (~200 m) similar to that observed in the video and is consistent with the debris length (x_d) of the staged analysis (see Table 2 and Fig. 6). The maximum thicknesses of debris at Ch 360 m and Ch 480 m calculated by LS-DYNA analysis are 3.5 and 2.5 m, respectively. The calculated values are similar to the maximum debris thickness estimated in the field, which is between 2 and 3 m (AECOM 2012).

The calibrated LS-DYNA model has been modified to include two intermediate barriers at Ch 360 m and Ch 480 m. The barriers are modelled using a rigid plate element, firmly attached to the topography. The barriers are 3 m high and assumed to be 2 m thick. The same material properties and resistance parameters as those adopted in the above calibration run are used. In contrast to staged analysis, LS-DYNA analysis simulates explicitly the dynamics of debris flows and debris retention behind intermediate barriers (see Fig. 7).

Figure 8 shows the velocity vector plots of the flow field in the proximity of the first intermediate barrier at Ch 360 m. The figure reveals the debris flow dynamics involved and the debris–barrier interaction. When the debris flow reaches the barrier, it is impeded by the obstruction of the barrier. Debris at the frontal portion runs up against the barrier. A plug is formed by the debris that is stopped and trapped behind the barrier. The extent of the plug develops when further debris is stopped behind the barrier. Debris flow subsequently rides on the plug and overtops the barrier. Debris overflowing from the barrier launches into a ballistic flight, and resumes its travel on the runout trail after landing.

Key results produced by the staged analysis and the LS-DYNA simulation are compared in Table 5. The adopted C_x value of the staged analysis is 0.8. The staged analysis generally gives results comparable to the LS-DYNA simulation, albeit on tghe relatively high side. The debris approaching velocity calculated by the staged analysis is 5% to 11% higher. Similarly, the thickness of the debris approaching barriers calculated by the staged analysis is greater when compared with the LS-DYNA analysis. In addition,

Fig. 6. Simulation of Yu Tung Road debris flow using LS-DYNA analysis.

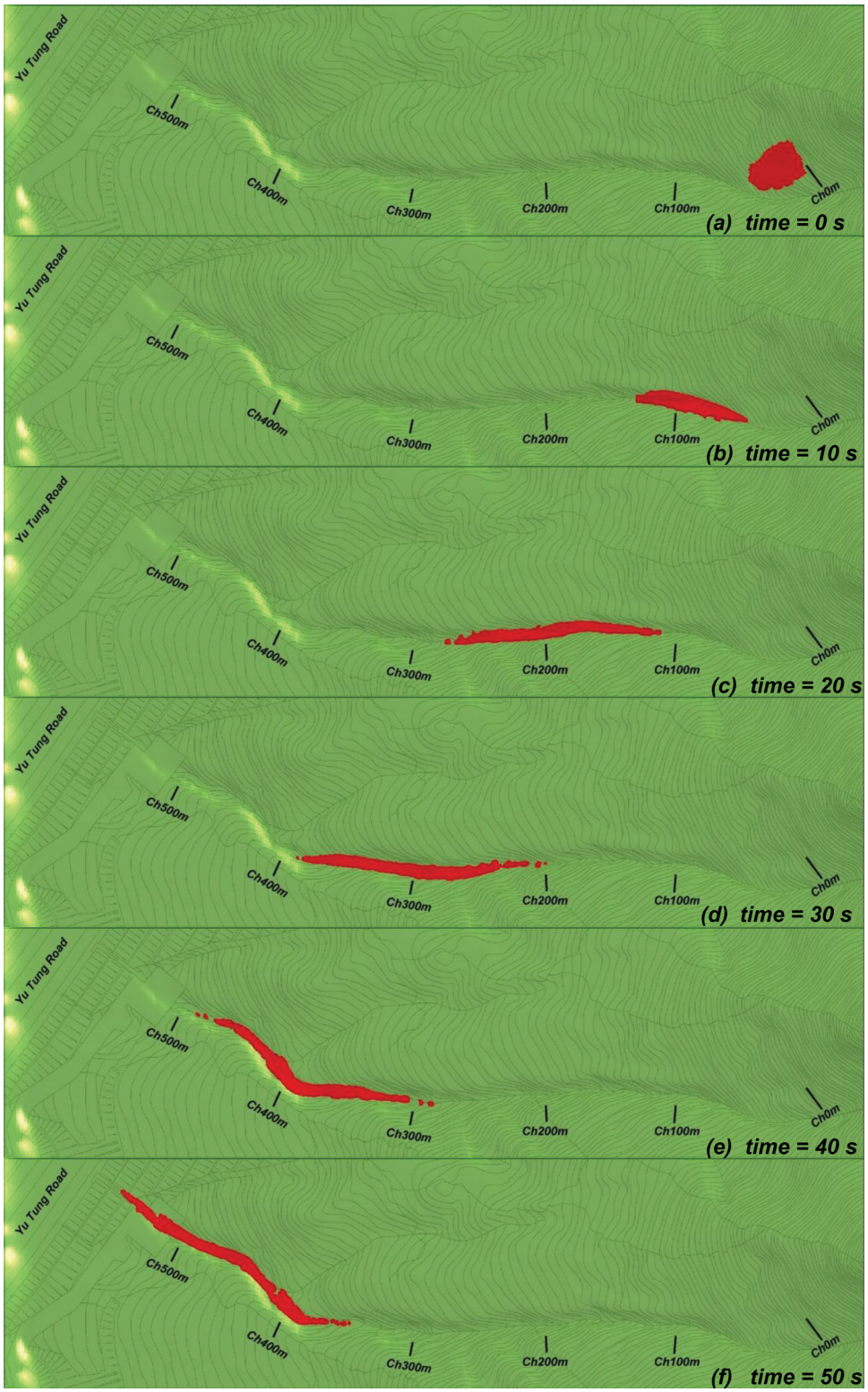

both LS-DYNA simulation and staged analysis give similar remaining kinetic energy of about 40% when compared with the free-field condition at the Ch 525 m location, i.e., about 60% of kinetic energy is dissipated by the two multiple barriers. Usually, a hydrodynamic equation would be used to calculate the dynamic impact pressure in sizing rigid barriers, where the pressure is proportional to the square of the velocity. For this illustrative example, the difference in dynamic impact pressure obtained from the velocities of 2d-DMM and LS-DYNA is 20% maximum, which is considered acceptable for the purpose of engineering design.

Two sets of additional analyses that assume intermediate barriers are 2 and 4 m high were carried out as a sensitivity study. It is observed that when smaller barriers of 2 m high are used, the debris impact thickness of the second and terminal barriers is

Fig. 7. Simulation of debris flow obstructed by multiple barriers.

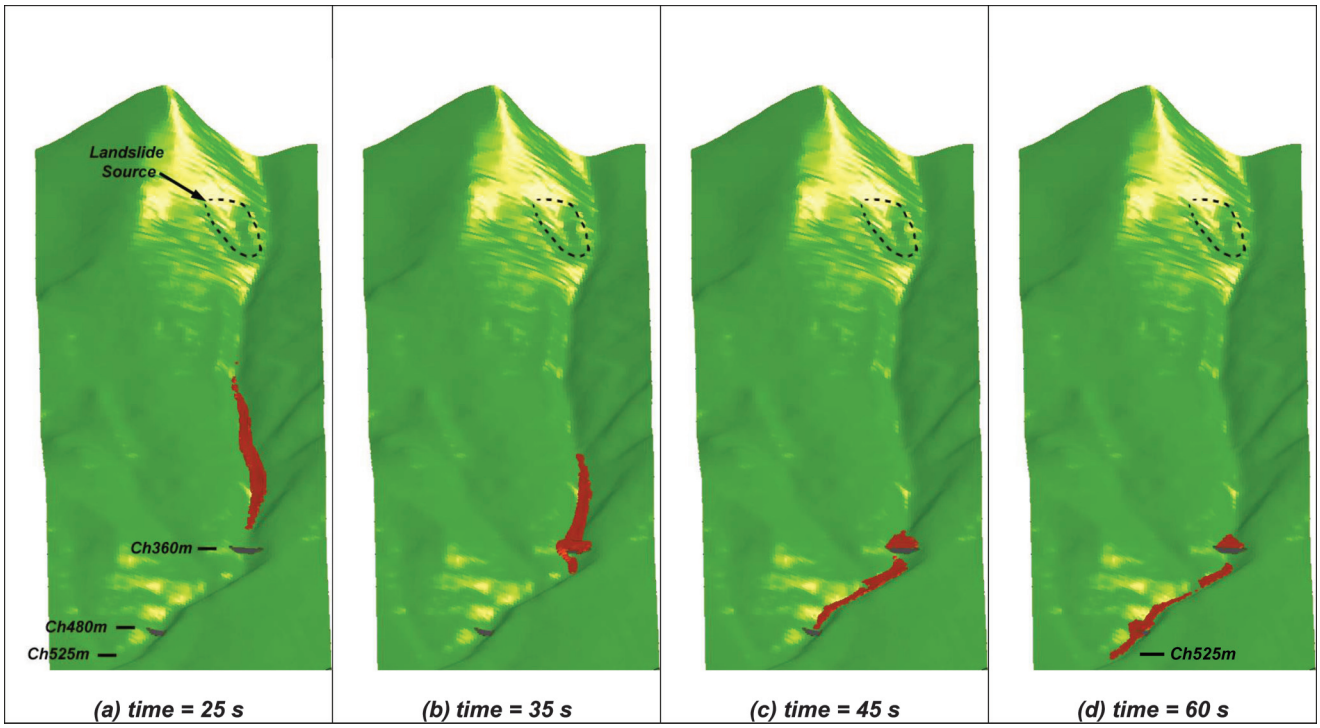

greater when compared with the 3 m high barriers, as the retention volume of the intermediate barrier is less. If higher intermediate barriers of 4 m high are used, the impact debris velocity and impact debris thickness of the second and terminal barriers reduce by 15% and 10%, respectively, because of the reduction in the mass of overflow debris from intermediate barriers.

A sensitivity analysis has also been carried out using different combinations of internal friction angles of 5° to 30°. It is noted that when internal friction angle does not exceed 20°, the effect of the internal friction angle on the calculated debris thickness is limited. However, when the internal friction angle is higher than 20°, the calculated debris thickness increases with the internal friction angle. The reason may relate to the internal pressure of the debris mass. The internal pressure reduces with the internal friction angle, and the reduced internal pressure tends to result in a more intact debris mass, i.e., less elongation and a thicker debris mass.

Discussion

For the Yu Tung Road site, the staged analysis and LS-DYNA simulation produce comparable results for design of multiple barriers, although the results of the staged analysis are relatively higher for the debris impact velocity and thickness. The results of the staged analysis can be adjusted to match LS-DYNA's output by lowering the value of the velocity correction factor R (see eq. (3)), as this will lead to a greater velocity reduction after landing. Nevertheless, calibration of the R value against LS-DYNA analysis for general use may not be appropriate because the R value would depend on the actual composition of the debris flow as well as the roughness and materials of the landslide trail at the debris landing location. The use of the recommended value of R (i.e., 0.7), which is on the high side of available data reported in literature, is selected with the intention of achieving a suitably robust design of debris-resisting barriers.

The staged analysis has been undertaken using the depth-averaged computer program. It is a simplified methodology for assessing dynamics of landslide debris that accounts for the obstruction of multiple barriers. Dynamic landslide simulations by the advanced numerical package LS-DYNA provide a more complete picture of debris mobility against the barriers. This could provide insights pertinent to the understanding of landslide debris–barrier interaction and could stimulate advancement in engineering design of mitigation measures against debris flows. Continuous research and development work including validation and calibration of three-dimensional numerical models for assessing landslide debris dynamics could bring positive impacts to engineering practice.

Two other observations can be made based on the present study:

1. *Height of intermediate barriers should not be excessive* — Debris overflowing from a barrier launches into a ballistic flight, and this debris gains potential energy and is not subject to any simultaneous basal resistance during the flight. The gain would increase when the debris runout path is steep, as a steeper runout profile would result in a larger drop height. To minimize the gain in potential energy, the barrier height should not be too large. Otherwise, the impedance to debris flow brought about by the intermediate barriers may be off-set and a net increase in kinetic energy of the landslide debris may result. Glassey (2013) also mentioned that the distance of debris overflow should be limited because it would induce an increase in velocity. The present study is useful for practitioners to consider the flow dynamics and overflow mechanism for an effective barrier height design.
2. *There is a time delay in debris flow reaching the outlet of a drainage line* — With the presence of multiple barriers, landslide debris may take longer to travel from the landslide source to the drainage outlet. The LS-DYNA simulation revealed that the Yu Tung Road debris flow might have reached the drainage outlet 50 s after the onset of the landslide (see Fig. 6*f*). With the presence of intermediate barriers, 10 more seconds would be required for the landslide debris to travel from the landslide source to the drainage outlet (see Fig. 8*d*; debris arrives at Ch 525 m at 60 s after landslide onsets). The additional time could be crucial in emergency situations because it could provide more lead time for affected people and traffic to take emergency actions (e.g., road closure using

Fig. 8. Simulation of debris flow velocity vector plots (barrier at Ch 360 m).

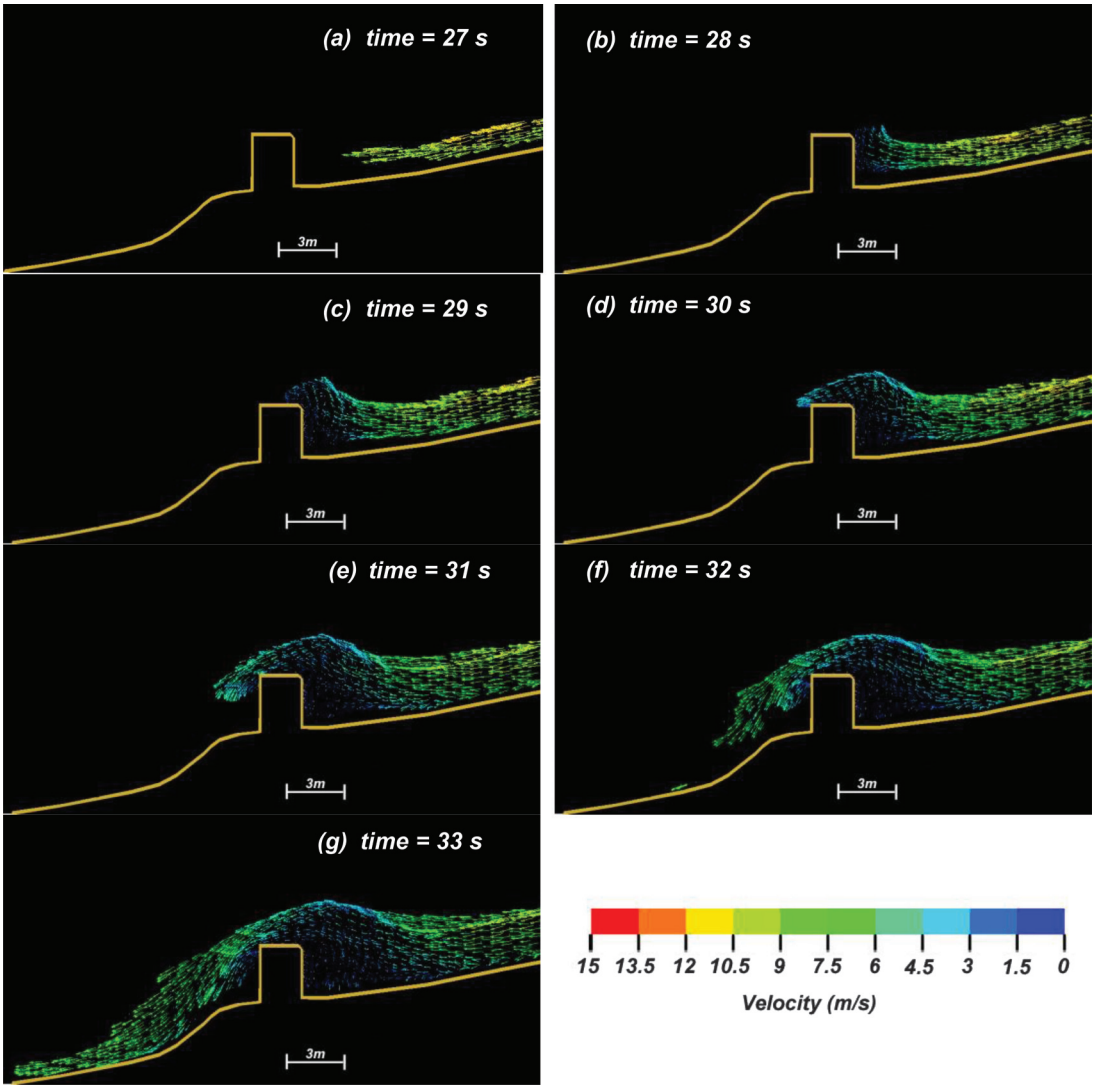

Table 5. Comparison between the results of the staged analysis and the LS-DYNA analysis.

	Ch 360 m		Ch 480 m		Terminal barrier	
	Debris approaching velocity (m/s)	Debris approaching thickness (m)	Debris approaching velocity (m/s)	Debris approaching thickness (m)	Debris approaching velocity (m/s)	Debris approaching thickness (m)
Staged analysis	12.0	2.8	8.3	1.9	7.5	1.1
LS-DYNA	11.0	1.5	7.9	1.1	6.7	1.0

automatic gate, etc.), albeit it appears to be limited. The time delay could be lengthened by placing additional intermediate barriers at suitable locations. With the installation of a system of sensors to detect impacts of landslide debris on intermediate barriers for provision of early warning, the multiple barrier scheme could be a robust mitigation measure for managing landslide risk.

Conclusions

A staged debris mobility analysis that considers the obstruction of multiple debris-resisting barriers has been proposed. The staged analysis makes use of Lagrangian depth-averaged solutions computed by a computer programs viz. DAN-W and 2d-DMM. The input parameters required for the staged analysis, e.g., correction factor to account for the velocity reduction at landing, have been established on the basis of available experimental data reported in literature and results of flume test of dry sand flows.

To illustrate the applicability of the staged analysis, the design debris impact thickness and velocity of a multiple barrier scheme to mitigate debris flow are calculated using the staged analysis. The results have been benchmarked with a three-dimensional dynamic landslide mobility assessment undertaken using LS-DYNA. The debris mobility model of LS-DYNA has been developed to consider turbulence resistance. Calibration of the LS-DYNA model is carried out using the debris velocity data corroborated by a video record and field mapping results. The results of the staged analysis and LS-DYNA assessment are comparable, although the staged analysis produces higher design parameters in general.

The dynamics of debris flows obstructed by barriers are complicated, involving filling up and overflowing of barriers. The sug-

gested staged mobility analysis is a simplified procedure that does not explicitly simulate these dynamics. The results generated are benchmarked with LS-DYNA analysis in one test site. Further review of the suitability of the staged analysis by means of field and laboratory experiments is worthwhile.

Acknowledgements

This paper is published with the permission of the Head of the Geotechnical Engineering Office and the Director of Civil Engineering and Development, Hong Kong SAR Government.

References

AECOM. 2012. Detailed study of the 7 June 2008 landslides on the hillside above Yu Tung Road, Tung Chung. GEO Report No. 271. Geotechnical Engineering Office, Hong Kong SAR Government.

ARUP. 2013. Pilot numerical investigation of the interactions between landslide debris and flexible debris-resisting barriers. Report prepared for Geotechnical Engineering Office, Hong Kong SAR Government. ARUP, Hong Kong.

Bertolo, P., and Wieczorek, G.F. 2005. Calibration of numerical models for small debris flows in Yosemite Valley, California, USA. Natural Hazards and Earth System Sciences, **5**: 993–1001. doi:10.5194/nhess-5-993-2005.

CGS. 2004. Design code for debris flow disaster mitigation measures, DZ/T0239-2004. (Draft). China Geological Survey. [In Chinese.]

Chan, Y.C., and Kwan, J.S.H. 2012. The state and practice of natural terrain landslide hazard mitigation in Hong Kong at 2012. *In* Proceedings of the One Day Seminar on Natural Terrain Hazard Mitigation Measures, Hong Kong. *Edited by* C.K. Lau, E. Chan, and J. Kwan. pp. 6–15.

Chen, X., Li, D., and Cui, P. 2009. Calculation buried depth of transverse sills for the debris flow drainage groove with soft foundation. Journal of Hefei University of Technology, **32**(10): 1590–1605. [In Chinese.]

Choi, C.E., and Ng, C.W.W. 2013. Flume tests to examine dynamics of debris flows obstructed by baffles. Final report. Report prepared for Geotechnical Engineering Office, Hong Kong SAR Government. The Hong Kong University of Science and Technology.

Crosta, G.B., Imposimato, S., and Roddeman, D. 2007. Approach to numerical modeling of long runout landslides. *In* Proceedings of the 2007 International Forum on Landslide Disaster Management. *Edited by* K. Ho and V. Li. Geotechnical Division, The Hong Kong Institution of Engineers. Vol. II, pp. 875–897.

GEO. 2011. Guidelines on the assessment of debris mobility for channelised debris flows. Technical Guidance Note No. 29. Geotechnical Engineering Office, Hong Kong SAR Government.

Glassey, T. 2013. Hydrology and check dams analysis in the debris flow context of Illgraben torrent. MAS Practical Research Project, Swiss Federal Institute of Technology, Zurich, Switzerland.

Hungr, O. 1995. A model for the runout analysis of rapid flow slides, debris flows, and avalanches. Canadian Geotechnical Journal, **32**(4): 610–623. doi:10.1139/t95-063.

Hungr, O., Morgenstern, N., and Wong, H.N. 2007. Review of benchmarking exercise on landslide debris runout and mobility modeling. *In* Proceedings of the 2007 International Forum on Landslide Disaster Management. *Edited by* K. Ho and V. Li. Geotechnical Division, The Hong Kong Institution of Engineers. Vol. II, pp. 755–812.

Iverson, R.M., Logan, M., and Denlinger, R.P. 2004. Granular avalanches across irregular three-dimensional terrain: 2. Experimental tests. Journal of Geophysical Research: Earth Surface (2003-2012), **109**: F01015. doi:10.1029/2003JF000084.

Kwan, J.S.H. 2012. Supplementary technical guidance on design of rigid debris-resisting barriers. Technical Note No. TN 2/2012. Geotechnical Engineering Office, Civil Engineering and Development Department, The HKSAR Government.

Kwan, J.S.H., and Sun, H.W. 2006. An improved landslide mobility model. Canadian Geotechnical Journal, **43**(5): 531–539. doi:10.1139/t06-010.

Kwan, J.S.H., Hui, T.H.H., and Ho, K.K.S. 2012. Modelling the motion of mobile debris flows in Hong Kong. *In* Landslide science and practice. Spatial analysis and modelling. *Edited by* C. Margottini, P. Canuti, and K. Sassa. Springer-Verlag Berlin Heidelberg, Vol. 3, pp. 29–35.

Kwan, J.S.H., Chan, S.L., Cheuk, J.C.Y., and Koo, R.C.H. 2014. A case study on an open hillside landslide impacting on a flexible rockfall barrier at Jordan Valley, Hong Kong. Landslides, **11**: 1037–1050. doi:10.1007/s10346-013-0461-x.

Liu, J., Nakatani, K., and Mizuyama, T. 2013. Effect assessment of debris flow mitigation works based on numerical simulation by using Kanako 2D. Landslides, **10**(2): 161–173. doi:10.1007/s10346-012-0316-x.

NILIM. 2007. Manual of technical standard for establishing sabo master plan for debris flow and driftwood. Technical Note of NILIM No. 364. Natural Institute for Land and Infrastructure Management, Ministry of Land, Infrastructure and Transport, Japan. [In Japanese.]

O'Brien, J.S., Julien, P.Y., and Fullerton, W.T. 1993. Two-dimensional water flood and mudflow simulation. Journal of Hydraulic Engineering, **119**(2): 244–261. doi:10.1061/(ASCE)0733-9429(1993)119:2(244).

Remaître, A., Van Asch, Th. W.J., Malet, J.-P., and Maquaire, O. 2008. Influence of check dams on debris-flow run-out intensity. Natural Hazards and Earth System Sciences, **8**: 1403–1416. doi:10.5194/nhess-8-1403-2008.

Roddeman, D.G. 2002. TOCHNOG user's manual – a free explicit/implicit FE program. FEAT. Available from www.feat.nl/manuals/user/user.html.

Shieh, C.L., Ting, C.H., and Pan, H.W. 2006. The impulsive force of debris flow on a curved dam. *In* Proceedings of the Interpraevent International Symposium on Disaster Mitigation of Debris Flows, Slope Failures and Landslides, Niigata, Japan. pp. 177–186.

Shum, L.K.W., and Lam, A.Y.T. 2011. Review of natural terrain landslide risk management practice and mitigation measures. Technical Note TN 3/2011. Geotechnical Engineering Office, The Civil Engineering and Development Department, The HKSAR Government.

Speerli, J., Hersperger, R., Wendeler, C., and Roth, A. 2010. Physical modeling of debris flows over flexible ring net barriers. *In* Proceedings of the Seventh International Conference on Physical Modelling in Geotechnics (ICPMG), Zurich, Switzerland. *Edited by* S. Springman, J. Laue, and L. Seward. Taylor & Francis Group. pp. 1285–1290.

SWCB. 2005. Soil and water conservation handbook. Soil and Water Conservation Bureau of the Council of Agriculture, Executive Yuan and Chinese Soil and Water Conservation Society. [In Chinese.]

Wendeler, C., Haller, B., and Salzmann, H. 2012. Protection against debris flows with 13 flexible barriers in the Milibach River (Canton Berne, Switzerland) and first event analysis. *In* Proceedings of the AGS Seminar on Natural Terrain Hazards Mitigation Measures, Hong Kong, 16 October 2012. *Edited by* C.K. Lau, E. Chan, and J. Kwan. The Association of Geotechnical and Geoenvironmental Specialists, Hong Kong. pp. 22–28. Available at http://ags-hk.org/notes/11/Proceedings_of_the_1_Day_Seminar_on_NTHMM_20121016.pdf.

White, D.J., Take, W.A., and Bolton, M.D. 2003. Soil deformation measurement using particle image velocimetry (PIV) and photogrammetry. Géotechnique, **53**: 619–631. doi:10.1680/geot.2003.53.7.619.

Wong, H.N. 2009. Rising to the challenges of natural terrain landslides. *In* Proceedings of the HKIE Geotechnical Division Annual Seminar 2009. Geotechnical Division, The Hong Kong Institution of Engineers. pp. 15–53.

WSL. 2008. Integral risk management of extremely rapid mass movements. Swiss Federal Institute for Snow and Avalanche Research. Available from http://irasmos.slf.ch/.

Yang, Q., Cai, F., Ugai, K., Yamada, M., Su, Z., Ahmed, A., Huang, R., and Xu, Q. 2011. Some factors affecting mass-front velocity of rapid dry granular flows in a large flume. Engineering Geology, **122**: 249–260. doi:10.1016/j.enggeo.2011.06.006.

Yang, Q., Cai, F., Ugai, K., Su, Z., Huang, R., and Xu, Q. 2012. A simple lumped mass model to describe velocity of granular flows in a large flume. Journal of Mountain Science, **9**: 221–231. doi:10.1007/s11629-012-2250-8.

Yiu, J., Pappin, J., Stuart, R., Kwan, J.S.H., and Ho, K.K.S. 2012. Landslide mobility and flexible barrier modeling using LS-DYNA. *In* Proceedings of AGS Seminar on Natural Terrain Hazards Mitigation Measures, 16 October 2012, Hong Kong. *Edited by* C.K. Lau, E. Chan, and J. Kwan. The Association of Geotechnical and Geoenvironmental Specialists, Hong Kong. pp. 67–77.

Appendix A. Flume test of landslide debris overflowing from rigid barrier

Testing was carried out in a 5 m long flume with a channel base width of 0.2 m. Side walls of this flume are about 0.5 m in height, perpendicular to the channel bed. Dry Leighton Buzzard Fraction C sand, composed of fairly uniform silica grains with a specific gravity of 2.65 g/cm^3, was used in this series of flume tests. The particle size of the sand ranges between 300 and 600 μm. The dynamic internal friction angle of the sand is 31° and the friction angle between the sand and flume bed is 23°. The initial bulk density of the sand mass is about 1680 kg/m^3. At the top end of the flume is a sand storage tank. Sand can be released into the flume by opening a flip gate that is attached to the tank. Details of the flume and sand release mechanism are presented in Choi et al. (2014).

The vertical barrier model used in the flume test is 0.1 m high and constructed using a 10 mm thick aluminum plate. It is firmly secured within the flume at the midway point of the channel. The scaling factor of the wall dimension is about 1/50 to the typical prototype.

Several trials were carried out to establish an appropriate flume inclination. It was subsequently decided that the flume should be inclined at 26° based on the consideration of the Froude number of the sand flow. The Froude number ($F_r = v/(gh)^{0.5}$, where v is debris velocity, g is gravitational acceleration, and h is debris depth normal to the flume bed) is a dimensionless parameter usually adopted to characterize the inertia of the debris flow. In design practice in Hong Kong, the value of F_r of debris flows in

Fig. A1. High-speed camera images (from Choi and Ng 2013).

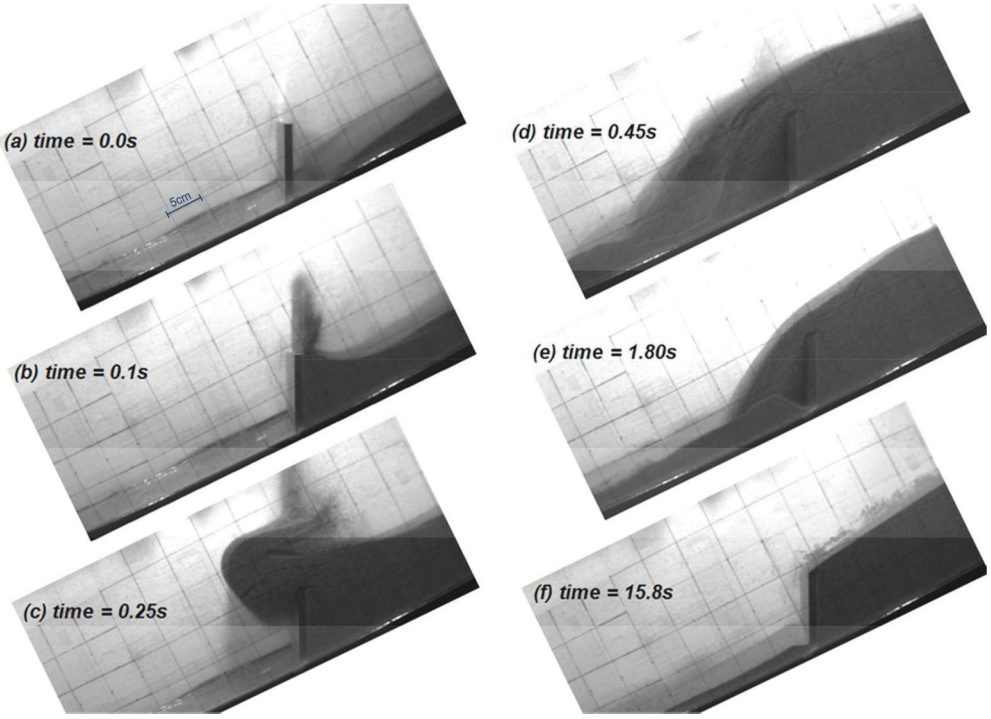

typical scenarios for barrier design is about 3, given that design impact velocity is about 10 m/s and the flow depth is about 1 m (i.e., $F_r = 10/(10 \times 1)^{0.5} = 3.2$). When the inclination of the flume is 26°, the sand flow in the flume would attain a velocity of about 2.6 m/s with an approaching depth of around 0.08 m at the location of the model barrier. This corresponds to a Froude number of 2.9 (= 2.6/(10 × 0.08)$^{0.5}$). A series of experiments with different source volumes of dry sand overflowing the rigid barrier has been carried out. The range of R factors observed from the experiments has been reported.

Experimental results

The flume test was recorded using a high-speed camera that could capture 100 images per second. Figure A1 shows the image records in sequence.

Figure A1*a* shows the instant when the dry sand flow arrived at the barrier location. For discussion purposes, the time of this instant is denoted as $t = 0.0$ s. After 0.1 s, the sand flow filled up the retention zone behind the barrier and splashing of the sand is also evident. At t = 0.25 s, debris that was not trapped behind the barrier started the overtopping process and launched into a ballistic flight. Subsequently, debris overflowing from the crest of the barrier travelled along a projectile path and landed on the flume bed at a distance about 0.2 m downstream of the barrier (see Fig. A1*d*). This process continued for about 16 s. At the end of the test, sand piled up behind the barrier and the deposition angle was about 33°.

In the present study, the velocity of the sand flow has been determined using the "geoPIV" computer package developed by White et al. (2003). This package is developed based on close-range photogrammetry techniques capable of tracking movements of soil grains captured in high-resolution images. It produces displacement and velocity vectors of the soil grains. Typical results of the PIV analysis are shown in Fig. 2.

Velocity reduction at landing

Velocity reduction immediately upon landing at the end of the ballistic flight has been studied. Table A1 summarizes the velocity parallel to the flume before and after landing as well as the velocity ratio. The velocity ratio ranges from about 0.3 to 0.5.

Table A1. Velocity data for calculating velocity reduction at landing.

Time (s)	Velocity parallel to flume just before landing, V_b (m/s)	Velocity parallel to flume immediately after landing, V_a (m/s)	V_a/V_b
0.46	1.3	0.6	0.46
0.51	1.4	0.6	0.43
0.61	1.6	0.7	0.44
1.11	1.6	0.4	0.25
1.31	1.3	0.4	0.31

Projectile length

Equation (1) is developed to calculate the length of projectile for debris overflowing from the crest of the barrier. The velocity and trajectory length data presented in Fig. 1 are used to verify this equation. As shown in the figure, debris overflowing velocity at the barrier crest is about 1.0 m/s. Using eq. (1), the estimated length of trajectory is 0.18 m. The trajectory length as observed in the test was 0.2 m. The difference of the trajectory length between the calculated value by eq. (1) and laboratory observation is within 10%, which is considered to be acceptable. However in reality, the predicted result may have a larger discrepancy, as the debris materials and scale of barriers could be quite different from the laboratory test.

References

Choi, C.E., and Ng, C.W.W. 2013. Flume tests to examine dynamics of debris flows obstructed by baffles. Final report. Report prepared for Geotechnical Engineering Office, Hong Kong SAR Government. The Hong Kong University of Science and Technology.

Choi, C.E., Ng, C.W.W., Song, D., Kwan, J.H.S., Shiu, H.Y.K., Ho, K.K.S., and Koo, R.C.H. 2014. Flume investigation of landslide debris-resisting baffles. Canadian Geotechnical Journal, **51**(5): 540–553. doi:10.1139/cgj-2013-0115.

White, D.J., Take, W.A., and Bolton, M.D. 2003. Soil deformation measurement using particle image velocimetry (PIV) and photogrammetry. Géotechnique, **53**: 619–631. doi:10.1680/geot.2003.53.7.619.

Fig. B1. Notations of different parameters relevant to debris overflows from barrier.

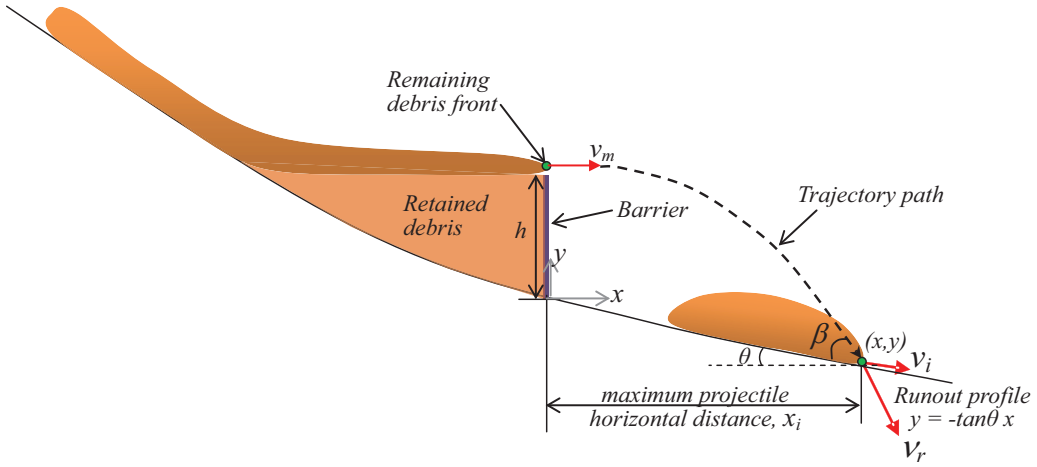

Fig. B2. Study of value of C_x.

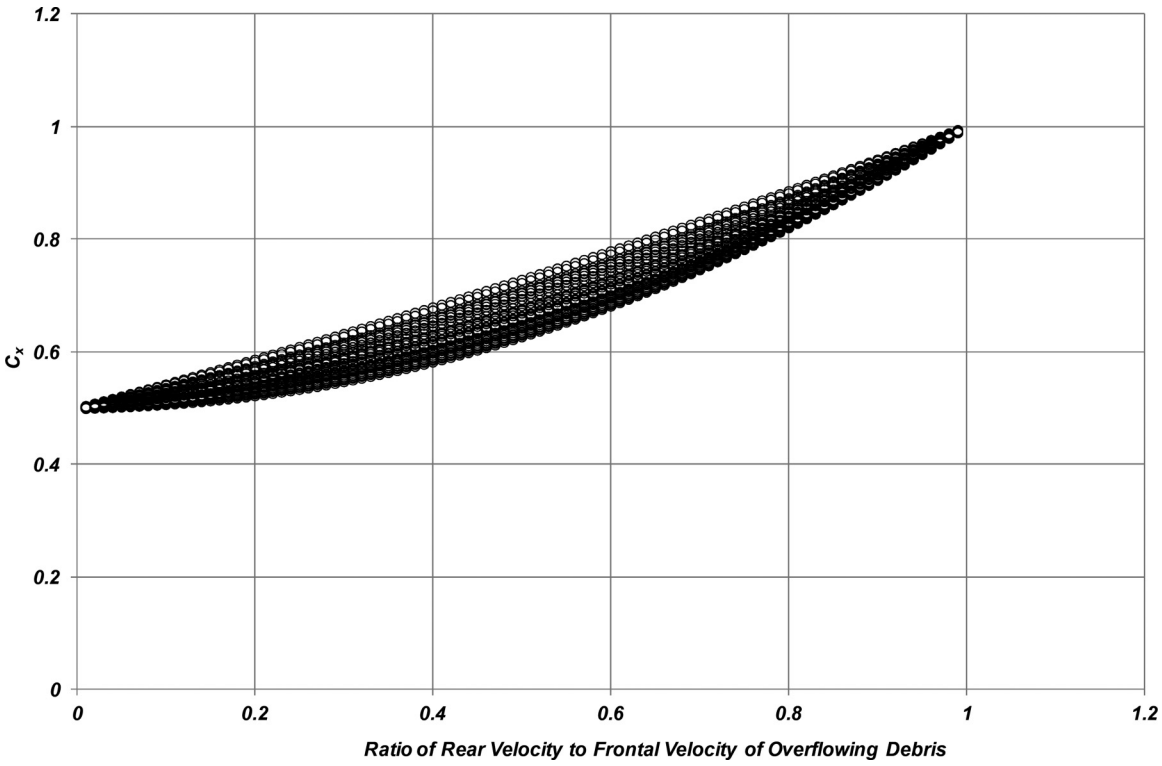

Appendix B. Derivation of eqs. (1) to (3)

Derivation of eq. (1) for calculation of x_i

Figure B1 shows notations of different parameters relevant to debris overflow from a barrier. The x-coordinate of the trajectory path of landslide debris is

(B1) $$x = v_m t$$

where t is time after debris launches from the barrier crest and v_m is the maximum velocity of debris that cannot be trapped by the barrier.

(B2) $$y = h - \tfrac{1}{2}gt^2$$

where g is gravitational acceleration.

To obtain the equation of the trajectory path of landslide debris, eq. (B1) is substituted into eq. (B2)

(B3) $$y = h - \tfrac{1}{2}g(x/v_m)^2$$

The equation of the runout path is

(B4) $$y = -\tan\theta\, x$$

Equations (B3) and (B4) are solved to obtain x_i

(B5) $$x_i = \frac{v_m^2}{g}\left(\tan\theta + \sqrt{\tan^2\theta + \frac{2gh}{v_m^2}}\right)$$

Derivation of eqs. (2) and (3) for calculation of v_r and v_i

v_r can be estimated based on the energy conservation principle, i.e.,

$$\text{(B6)} \qquad \tfrac{1}{2}m_r v_r^2 = \mathrm{KE}_1 - \mathrm{KE}_2 + m_r g(h + C_x x_i \tan\theta)$$

where m_r is the mass of debris overflow from the barrier, v_r is the velocity of the remaining debris just before landing, KE_1 is the total kinetic energy of the debris before being intercepted by the barrier, and KE_2 is the kinetic energy of debris retained by the barrier.

The last term in eq. (B6) corresponds to potential energy gained in the ballistic flight. x_i is the horizontal distance that the landslide debris could travel; it is calculated using the maximum velocity of debris overflowing from the barrier (see eq. (B1)). As the ratio of rear velocity to frontal velocity of the overflowing debris varies, a correction factor C_x is proposed to establish an average value of x_i relevant to the energy calculation. The value of C_x depends on the ratio of the rear and frontal velocities of the overflowing debris, and can be calculated using eq. (B5) based on a combination of selected barrier height, debris velocity, and inclination of the runout profile with consideration of different velocity ratios. The leading portion of the debris flow typically has the highest velocity and kinetic energy. Therefore, the minimum spacing between barriers (x_i) should be calculated using the debris frontal velocity as presented in this study. However, the velocity of the rear portion of the overflow debris would be much slower. The use of the highest debris velocity as the initial condition of the debris mobility analysis of the next stage would result in a gross overestimation of the impact on the barrier downstream. It is suggested that the overflow kinetic energy not be designed too conservatively to avoid oversizing of the barriers. As, the attenuation of overflow debris mobility would be considered. Figure B2 shows a plot of C_x versus velocity ratio. The data are generated based on combinations of a range of debris velocity up to 15 m/s, barrier heights of 1 to 5 m, and runout path inclinations of 20° to 60°. Values of C_x that envelop the upper limit of the data are recommended for use in the staged analysis (see also Table 1).

Equation (B6) can be simplified to the following form:

$$\text{(B7)} \qquad v_r = \sqrt{\frac{2[\mathrm{KE}_r + m_r g(h + C_x x_i \tan\theta)]}{m_r}}$$

where $\mathrm{KE}_r = \mathrm{KE}_1 - \mathrm{KE}_2$ (i.e., the kinetic energy of the overflow debris that can be obtain from debris mobility analysis).

v_r is the velocity of the remaining debris just before landing; it is in a direction tangential to the trajectory path. The velocity for inputting to the dynamic analysis of landslide debris at the next stage (i.e., debris velocity after landing, v_i) is parallel to the inclination of the runout profile, which can be calculated as follows.

With β denoted as the angle between v_r and the debris runout path (see Fig. B1), $\beta + \theta$ is the inclination of v_r to horizontal, i.e.,

$$\text{(B8)} \qquad \beta + \theta = \tan^{-1}\sqrt{\frac{m_r g(h + C_x x_i \tan\theta)}{\mathrm{KE}_r}}$$

and

$$\text{(B9)} \qquad v_i = v_r \cos\beta$$

Combining eqs. (B8) and (B9) and applying the velocity reduction factor (R) to account for the velocity reduction at landing, eq. (B10) is obtained

$$\text{(B10)} \qquad v_i = R v_r \cos\left\{\left[\tan^{-1}\sqrt{\frac{m_r g(h + C_x x_i \tan\theta)}{\mathrm{KE}_r}}\right] - \theta\right\}$$